



JOINT INSTITUTE FOR NUCLEAR RESEARCH
Frank Laboratory of Neutron Physics

FINAL REPORT
INTEREST (Wave 7)

“Coexistence of superconductivity and ferromagnetism at low-dimensional heterostructures”

Supervisor:

Dr. V. Zhaketov

Student:

Zaky Abdelslam Zaky Ebrahim
(Faculty of Science Beni-Suef University, Egypt)

Participation period:

13 June -22 July

2022

Contents:

Cover page	1
Contents	2
1. Acknowledgment	3
2. Abstract	4
3. Introduction.	4
4. Materials and structure	6
5. Results and discussion	8
6. Conclusion and future work.	13
7. References.	13

Acknowledgment

I would like to thank Dr. Vladimir Zhaketov for his assistance and his fruitful discussions. Also, I express our deepest gratitude to both the ASRT and JINR committee for giving us this great opportunity to learn, not only academically, but also, on a social and personal level.



Coexistence of superconductivity and ferromagnetism at low-dimensional heterostructures

Abstract

In this project, polarized neutron reflectometry is used to investigate ferromagnetic and antiferromagnetic heterostructures. The proposed heterostructures are $\text{Al}_2\text{O}_3/\text{Cr}/[\text{Fe}/\text{Cr}]_{12}/\text{Gd}/\text{Cr}$ and $\text{Al}_2\text{O}_3/\text{Nb}/[\text{Fe}/\text{Nb}]_{12}/\text{Nb}$. Neutron reflectivity is calculated for both theoretical and experimental data.

Introduction

Artificial periodic and non-periodic structures have gotten a lot of interest recently [1-12]. The coexistence of superconductivity, ferromagnetism, and antiferromagnetism (S, F, and AF) systems in uniform materials is very sensitive and needs special conditions due to the paramagnetic effect. The paramagnetic effect is the suppression of S because of the exchange field in F. The concentrated magnetic field lines of F are expelled with S as a result of the Meissner effect [13-15]. When the exchange field of F causes Zeeman energy with a higher value than the coupling energy between Cooper pairs, S is destroyed. Besides, the exchange fields re-align the spin Cooper pairs to be parallel to each other. For S/F heterostructures at certain conditions, proximity and magnetic proximity effects appear at each S/F interface due to the mutual interaction between them [16, 17].

Superconducting spintronics is an attractive field that manipulates the spin degrees of freedom in condensed-matter systems [18]. The term "spin" refers to the single electron spin or the average spin of a group of electrons, as represented by magnetization. The spin can be controlled by either its phase and population or by manipulating the spin of one or more spin systems [19]. Without inversion symmetry, the spin-orbit interplay in ferromagnetic layers provides a probability for a linear coupling between the magnetic moment and the supercurrent (I_s) in Josephson junctions (JJs) of S/F/S [20]. In 1962, Brian Josephson discovered the Josephson effect

[21]. He predicted that I_s can be existed between two superconductor layers separated by a thin layer of insulator. In the second year, Anderson and Rowell stationary observed Josephson effect experimentally for the first time [22]. The discovery of the JJ has contributed to the development of different types of sensors for detecting very weak magnetic fields and electromagnetic radiation [23].

As clear in Fig.1, Khaydukov et al. [12] investigated experimental S/F superlattices terminated by a relatively thick Nb layer. A Standard four-point contact method was used to measure the resistivity. The residual resistivity ratio of the prepared samples under these conditions is very high (15–20). The sample produced a depth modulated alloy of FeNb with an iron content ranging between 60% and 90%. The ferromagnetic characteristics of this alloy are poor.

The proximity effect of this weak ferromagnetic behavior of FeNb alloy to the thick cap layer of Nb superconductor results in an intermediate phase defined by suppressed but still limited structural resistance in a temperature interval of roughly 1 K below the thick Nb superconducting transition. The authors used X-ray diffraction (XRD) to evaluate the epitaxial growth quality and crystal structure. Guasco et al. [1] reported an experimental design composed of Nb/Co/Nb. Using PNR, they proposed direct, fast, non-destructive and sensitive measurements to detect the concentration of hydrogen in thin films.

In 2014, Li et al. [24] studied the exchange-spring behavior of the LSCO/LSMO bilayer. They observed an unexpected behavior of magnetic switching that differs from that of traditional exchange-spring structures. In 2019, Koohfar et al. [25] experimentally designed [LSCO(2)/LSMO(2)] heterostructure to evaluate the magnetic moment inside them. LSMO is magnetically soft F, but LSCO is magnetically hard F. In 2002, Lauter et al. [26] studied Fe/Cr multilayer structure and obtained that the Fe magnetization is twisted through the multilayer stack proving a stable noncollinear configuration.

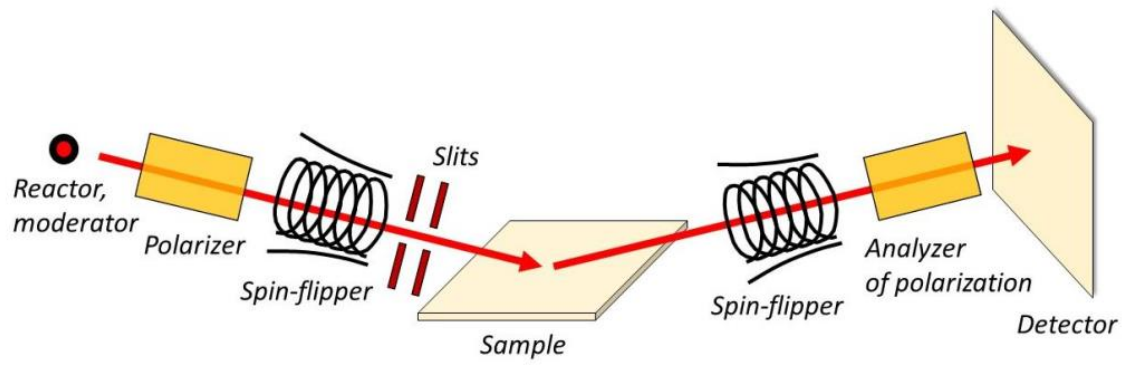


Fig.1: Classical polarized neutron reflectometer setup.

Materials and structure:

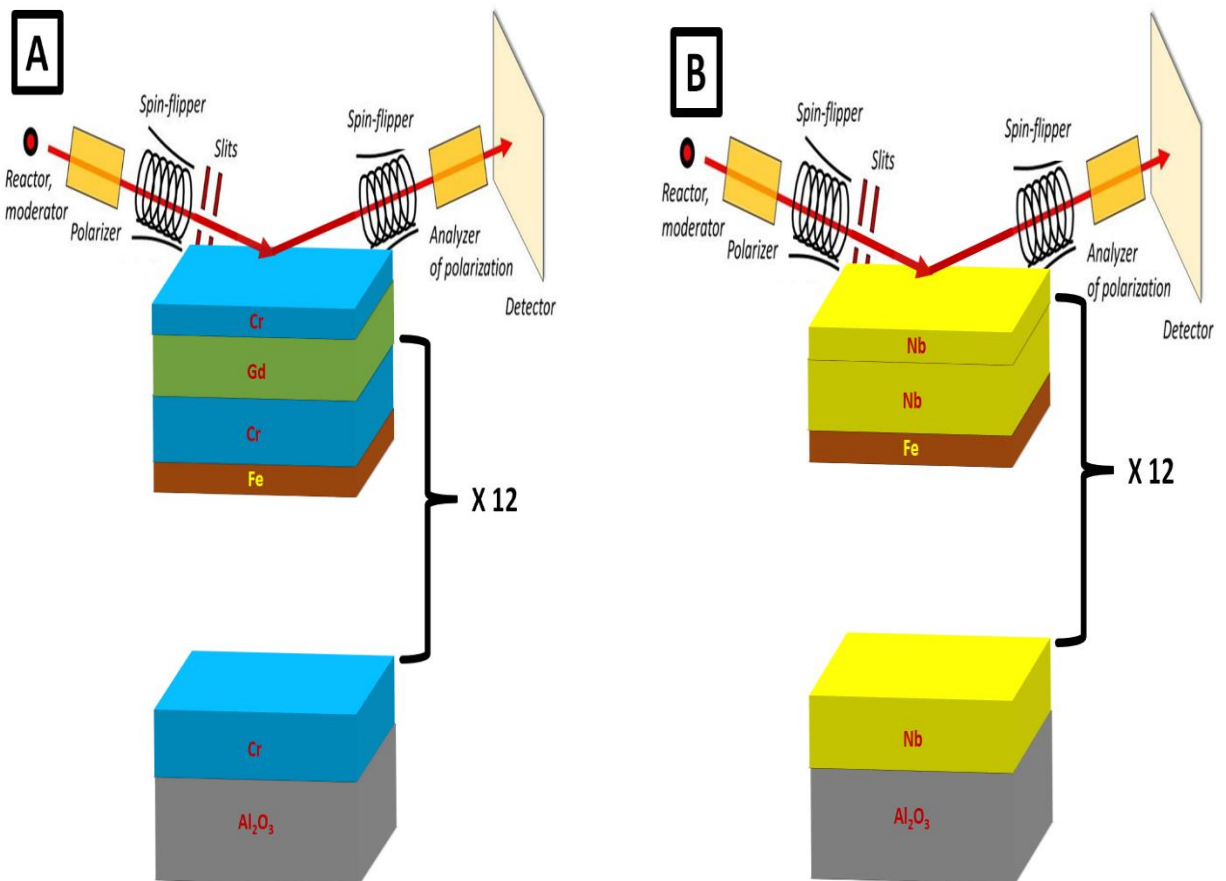


Fig. 2: Schematic of PNR experiment setup and sample with deposited layers (A) $\text{Al}_2\text{O}_3/\text{Cr}_1/ [\text{Fe}/\text{Cr}_2] \times 12 / \text{Gd}/\text{Cr}_3$, (B) $\text{Al}_2\text{O}_3/\text{Nb} / [\text{Fe} / \text{Nb}] \times 12 / \text{Nb}$.

Polarized neutron reflectometry (PNR) is a very distinguished depth-resolved

technique that offers a one-of-a-kind way of "viewing" vector magnetization with incredibly high quality and spatial resolution. This technique depends on the interplay between the magnetic moments of both neutron and structure. Because neutrons have a magnetic moment, and their wavelengths can be adjusted to be comparable to interatomic distances, they undergo a simple dipole-dipole interaction in addition to the ordinary short-range nuclear interaction when they are scattered by a magnetic moment of an atom. Depending on whether the neutron's spin state changes ("flips"), the reflectivities of reflected neutron beams from a magnetic film can be distinguished. Due to the ability of PNR to measure the vector magnetization profile of magnetic films, periodic or non-periodic structures of ferromagnetic films separated by other materials can be examined to investigate their different magnetic behaviors. By studying the non-specular and specular spin-dependent scattering, the impact of thin layer thickness or magnetic domain orientation and size can be performed [27]. Because the wavelength of the thermal neutron is comparable to the London penetration depth and coherent length of ferromagnet and superconductor films, neutron beams are particularly well suited to investigating S/F systems.

The proposed structures are $\text{Al}_2\text{O}_3/\text{Cr}/ [\text{Fe}/\text{Cr}]_{12} / \text{Gd}/\text{Cr}$ and $\text{Al}_2\text{O}_3/\text{Nb} / [\text{Fe} / \text{Nb}]_{12} / \text{Nb}$ on sapphire substrates (Al_2O_3) with an area of $10 \times 10 \text{ mm}^2$. Molecular beam epitaxy is used to grow thin films of Nb. Besides, PNR will be carried out to study the vector magnetization of the structure.

Results and discussion:

Firstly, the interaction between neutron beam and $\text{Al}_2\text{O}_3/\text{Cr}_1(100 \text{ \AA}) / [\text{Fe}(90 \text{ \AA}) / \text{Cr}_2(11 \text{ \AA})]_{\times 12} / \text{Gd}(50 \text{ \AA}) / \text{Cr}_3(50 \text{ \AA})$ structure will be studied. The grazing angle is 8.76 mrad and the magnetization $M_z = 24 \text{ Oe}$. As clear in Fig. 3, the neutron reflectivity R_{++} and R_{--} record low reflectivity at low wavelengths. By increasing the wavelength of the incident neutrons, the reflectivity gradually increases until it reached the maximum reflectivity at λ of about 6 \AA . By using the theoretical model, the simulated data has higher reflectivity. Due to the fabrication tolerance, we will fit the parameters within the range of $\pm 30 \%$.

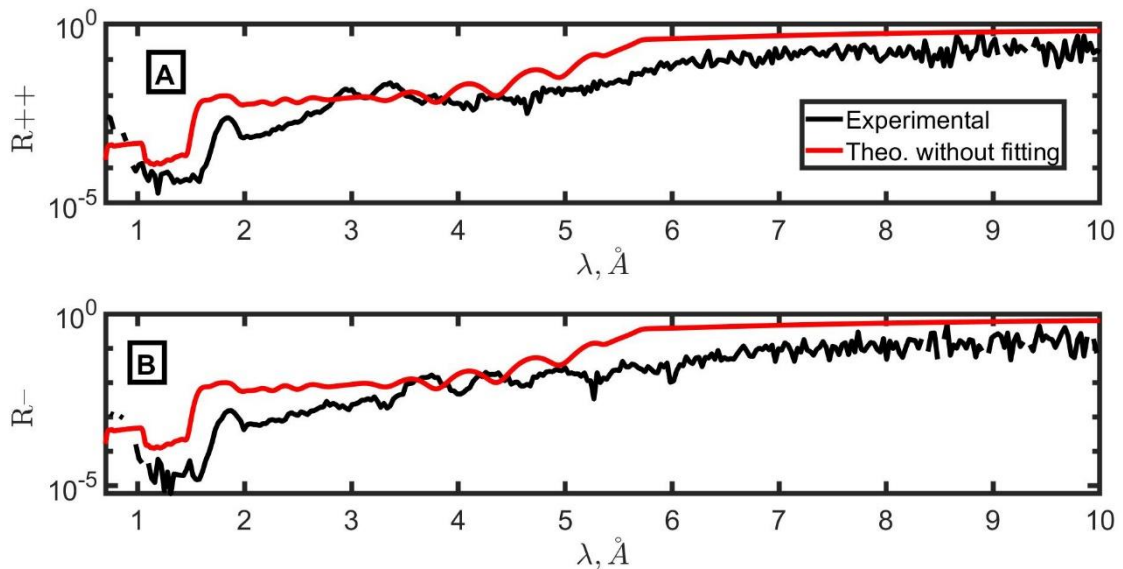


Fig. 3: Neutron reflectivities (A) R_{++} , (B) R_{--} for $\text{Al}_2\text{O}_3/\text{Cr}_1(100 \text{ \AA}) / [\text{Fe}(90 \text{ \AA}) / \text{Cr}_2(11 \text{ \AA})]_{\times 12} / \text{Gd}(50 \text{ \AA}) / \text{Cr}_3(50 \text{ \AA})$ structure at a grazing angle of 8.76 mrad and external magnetic field of 24Oe.

Now, we will study the fabrication tolerance of the thickness of Cr_3 within the range of $\pm 30 \%$ (from 35 \AA to 65 \AA). As clear in Fig. 5, the thickness of 35 \AA is the closest one to the experimental data compared with the other values. So, we will complete other fitting processes with $\text{Cr}_3 = 35 \text{ \AA}$.

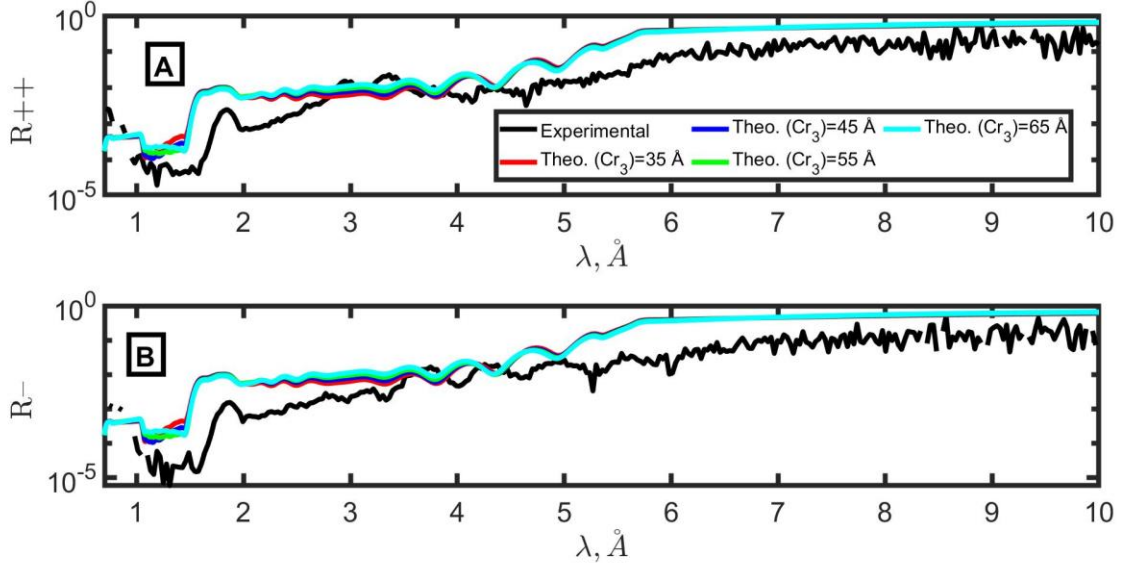


Fig. 4: Neutron reflectivities (A) R_{++} , (B) R_{--} for $\text{Al}_2\text{O}_3/\text{Cr}_1(100 \text{ \AA}) / [\text{Fe}(90 \text{ \AA}) / \text{Cr}_2(11 \text{ \AA})] \times 12 / \text{Gd}(50 \text{ \AA}) / \text{Cr}_3(50 \text{ \AA})$ structure at a grazing angle of 8.76 mrad and external magnetic field of 240e for different values of Cr_3 thickness.

By studying the fabrication tolerance of the thickness of Gd within the range of $\pm 30 \%$ (from 35 \AA to 65 \AA), a thickness of 65 \AA seems to be better than other thicknesses, as clear in Fig. 5.

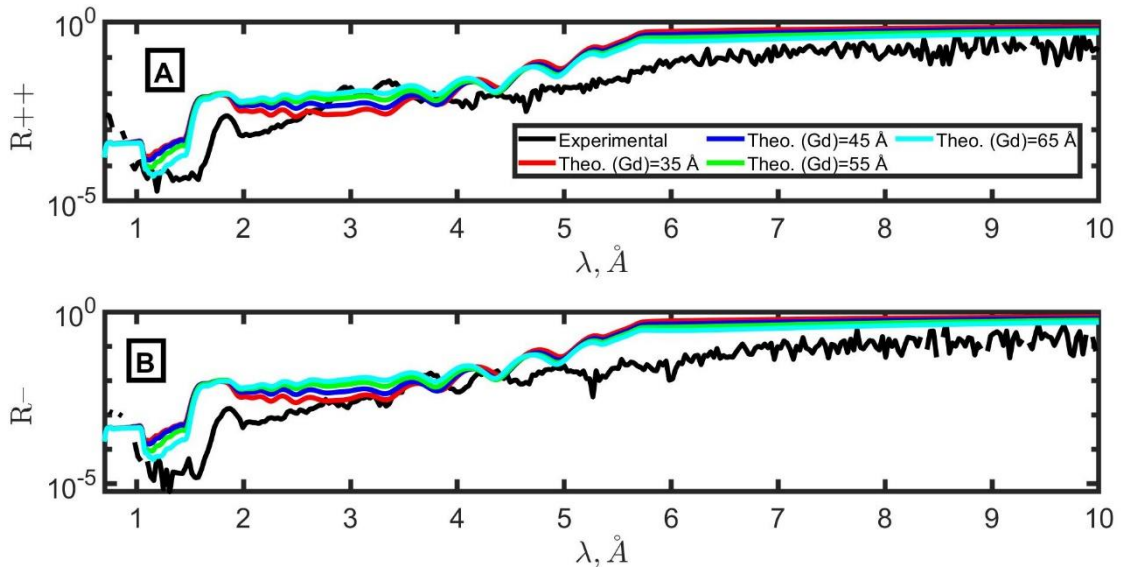


Fig. 5: Neutron reflectivities (A) R_{++} , (B) R_{--} for $\text{Al}_2\text{O}_3/\text{Cr}_1(100 \text{ \AA}) / [\text{Fe}(90 \text{ \AA}) / \text{Cr}_2(11 \text{ \AA})] \times 12 / \text{Gd}(50 \text{ \AA}) / \text{Cr}_3(50 \text{ \AA})$ structure at a grazing angle of 8.76 mrad and external magnetic field of 240e for different values of Gd thickness.

After that, the thickness of Cr₂ within the range of $\pm 30\%$ (from 7.7 Å to 14.3 Å) will be studied. We found that the Cr₂ thickness of 11 Å is relatively good, as clear in Fig. 6. For the Fe layer, the range of $\pm 30\%$ (from 63 Å to 117 Å) is studied as clear in Fig. 7. We will select the thickness of 103.5 Å.

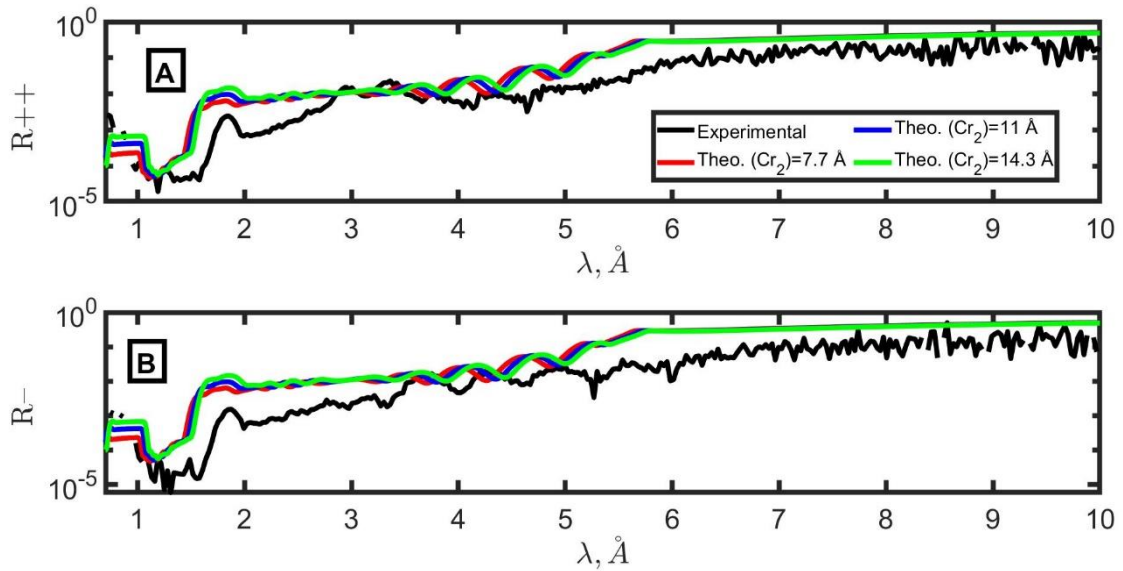


Fig. 6: Neutron reflectivities (A) R₊₊, (B) R₋₋ for Al₂O₃/Cr₁(100 Å) / [Fe(90 Å) / Cr₂(11 Å)]x12 / Gd(50 Å) / Cr₃(50 Å) structure at a grazing angle of 8.76 mrad and external magnetic field of 240e for different values of Cr₂ thickness.

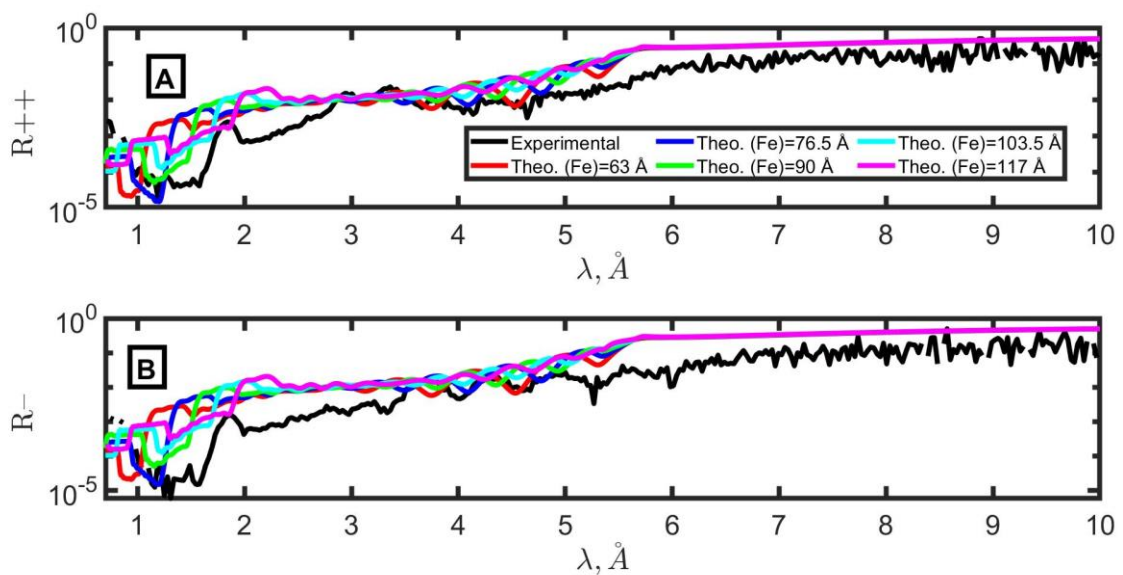


Fig. 6: Neutron reflectivities (A) R₊₊, (B) R₋₋ for Al₂O₃/Cr₁(100 Å) / [Fe(90 Å) / Cr₂(11 Å)]x12 / Gd(50 Å) / Cr₃(50 Å) structure at a grazing angle of 8.76 mrad and external

magnetic field of 240e for different values of Fe thickness.

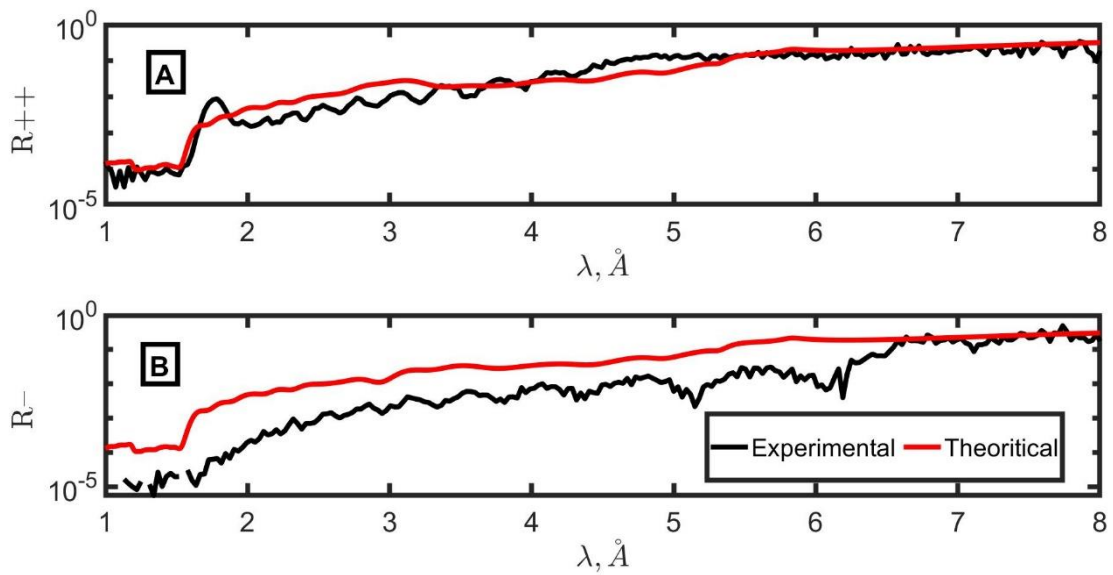


Fig. 4: Neutron reflectivities (A) R_{++} , (B) R_{--} for $\text{Al}_2\text{O}_3/\text{Cr}/[\text{Fe}/\text{Cr}]^*12/\text{Gd}/\text{Cr}$ structure at a grazing angle of 8.76 mrad and external magnetic field of 4 kOe.

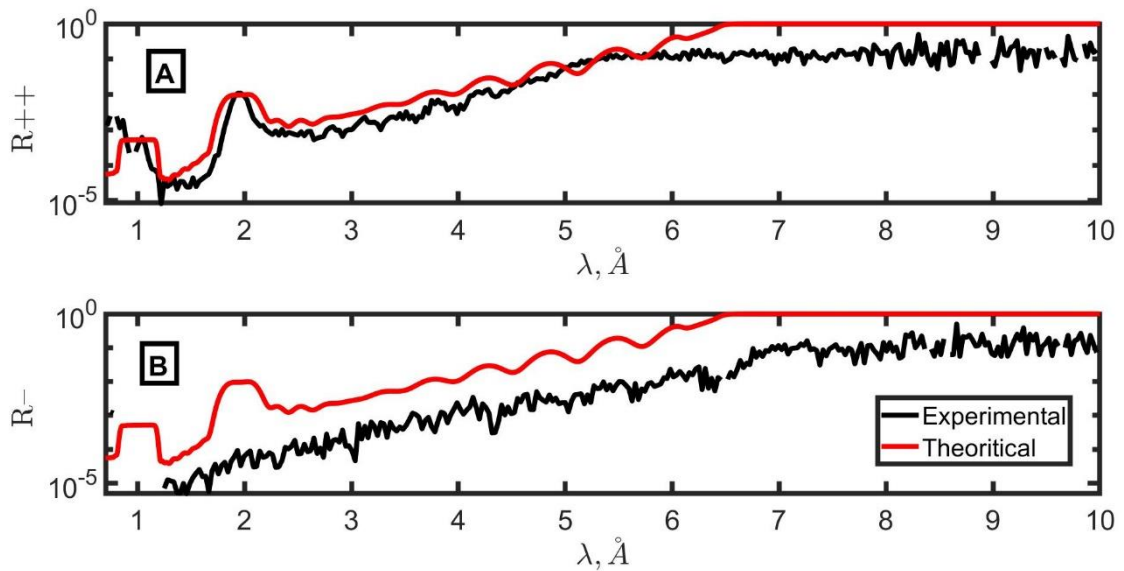


Fig. 5: Neutron reflectivities (A) R_{++} , (B) R_{--} for $\text{Al}_2\text{O}_3/\text{Nb}/[\text{Fe}/\text{Nb}]^*12/\text{Nb}$ structure at a grazing angle of 9.25 mrad and external magnetic field of 240e.

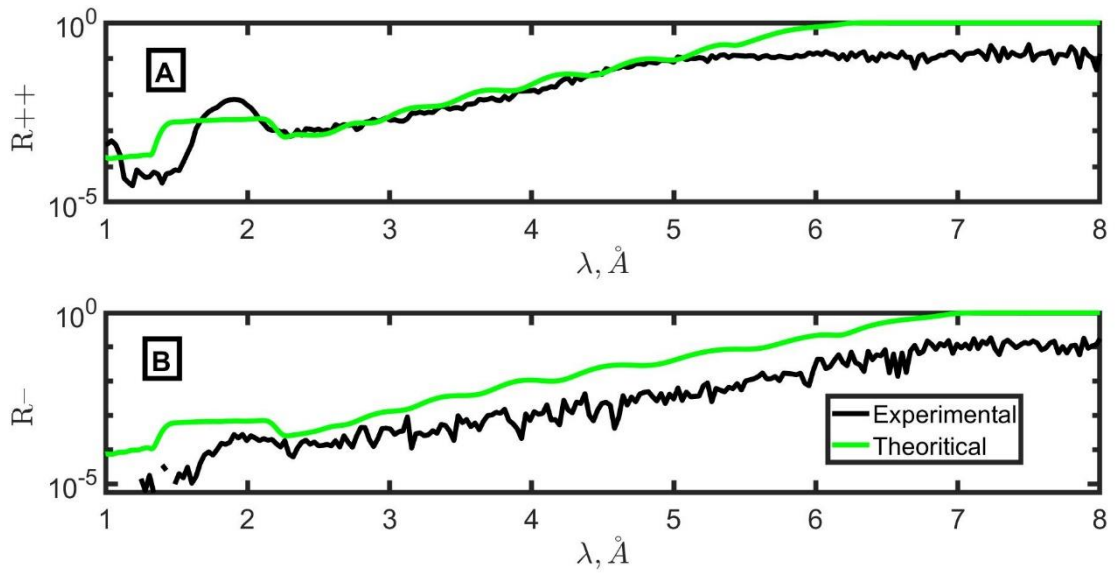


Fig. 6: Neutron reflectivities (A) R_{++} , (B) R_{--} for $\text{Al}_2\text{O}_3/\text{Nb}/[\text{Fe}/\text{Nb}]^*12/\text{Nb}$ structure at a grazing angle of 9.25 mrad and external magnetic field of 4 kOe.

Conclusion and future work

In this report, we plotted the experimental data of two structures. Then, we fitted these structures theoretically. Due to the small period of this interesting wave (6 weeks), we will complete the fitting process in the future. After that, we will discuss and explain the results.

References

1. L. Guasco, Y. N. Khaydukov, S. Pütter, L. Silvi, M. Paulin, T. Keller, and B. Keimer, "Resonant neutron reflectometry for hydrogen detection," *Nat. Commun.* **13**, 1486 (2022). <https://doi.org/10.1038/s41467-022-29092-z>
2. Z. A. Zaky, A. M. Ahmed, A. S. Shalaby, and A. H. Aly, "Refractive index gas sensor based on the Tamm state in a one-dimensional photonic crystal: Theoretical optimisation," *Sci. Rep.* **10**, 9736 (2020). <https://doi.org/10.1038/s41598-020-66427-6>
3. E. Yakunina, E. Kravtsov, Y. N. Khaydukov, N. Antropov, and V. Proglyado, "Synthesis, Structure and Magnetic Properties of Multilayer Nanoheterostructures Fe| MgO| Cr| MgO| Fe," *Physics of the Solid State* **63**, 1584-1587 (2021). <https://doi.org/10.1134/S1063783421090456>
4. Z. A. Zaky and A. H. Aly, "Modeling of a biosensor using Tamm resonance excited by graphene," *Appl. Optics* **60**, 1411-1419 (2021). <https://doi.org/10.1364/AO.412896>
5. M. Makarova, E. Kravtsov, A. Pavlova, V. Ustinov, and Y. Khaydukov, "Magnetic Structure of Planar Dy/Co Nanoheterostructures at Room Temperature," *Journal of Surface Investigation: X-ray, Synchrotron and Neutron Techniques* **15**, 966-969 (2021). <https://doi.org/10.1134/S1027451021040327>
6. Z. A. Zaky and A. H. Aly, "Gyroidal graphene/porous silicon array for exciting optical Tamm state as optical sensor," *Sci. Rep.* **11**, 19389 (2021). <https://doi.org/10.1038/s41598-021-98305-0>
7. Z. A. Zaky, A. Sharma, S. Alamri, and A. H. Aly, "Theoretical evaluation of the refractive index sensing capability using the coupling of Tamm–Fano resonance in one-dimensional photonic crystals," *Appl. Nanosci.* **11**, 2261–2270 (2021). <https://doi.org/10.1007/s13204-021-01965-7>
8. Z. A. Zaky, A. Sharma, and A. H. Aly, "Gyroidal Graphene for Exciting Tamm Plasmon Polariton as Refractive Index Sensor: Theoretical Study," *Opt. Mater.* **122**, 111684 (2021). <https://doi.org/10.1016/j.optmat.2021.111684>
9. Z. A. Zaky, M. R. Singh, and A. H. Aly, "Tamm resonance excited by different metals and graphene," *Photonics Nanostruct.* **49**, 100995 (2022). <https://doi.org/10.1016/j.photonics.2022.100995>
10. Z. A. Zaky, A. Panda, P. D. Pukhrambam, and A. H. Aly, "The impact of magnetized cold plasma and its various properties in sensing applications," *Sci. Rep.* **12**, 3754 (2022). <https://doi.org/10.1038/s41598-022-07461-4>
11. E. Benckiser, Y. Khaydukov, L. Guasco, K. Fürsich, P. Radhakrishnan, G. Kim, and B. Keimer, "Complementary Insights from Neutron and Resonant X-Ray Reflectometry for the Study of Perovskite Transition Metal Oxide Heterostructures," *physica status solidi (b)* **259**, 2100253 (2022). <https://doi.org/10.1002/pssb.202100253>
12. Y. Khaydukov, S. Pütter, L. Guasco, R. Morari, G. Kim, T. Keller, A. Sidorenko, and B. Keimer, "Proximity effect in [Nb (1.5 nm)/Fe (x)] 10/Nb (50 nm) superconductor/ferromagnet heterostructures," *Beilstein journal of nanotechnology* **11**, 1254-1263 (2020). <https://doi.org/10.3762/bjnano.11.109>
13. Y. A. Izyumov, Y. N. Proshin, and M. G. Khusainov, "Competition between superconductivity and

- magnetism in ferromagnet/superconductor heterostructures," *Physics-Uspekhi* **45**, 109 (2002).<https://doi.org/10.1070/PU2002v045n02ABEH001025>
14. A. I. Buzdin, "Proximity effects in superconductor-ferromagnet heterostructures," *Reviews of modern physics* **77**, 935 (2005).<https://doi.org/10.1103/RevModPhys.77.935>
 15. R.-G. Cai and R.-Q. Yang, "Coexistence and competition of ferromagnetism and p-wave superconductivity in holographic model," *Physical Review D* **91**, 026001 (2015).<https://doi.org/10.1103/PhysRevD.91.026001>
 16. Y. N. Khaydukov, E. Kravtsov, V. Zhaketov, V. Progliado, G. Kim, Y. V. Nikitenko, T. Keller, V. Ustinov, V. Aksenov, and B. Keimer, "Magnetic proximity effect in Nb/Gd superlattices seen by neutron reflectometry," *Phys. Rev. B* **99**, 140503 (2019).<https://doi.org/10.1103/PhysRevB.99.140503>
 17. Y. N. Khaydukov, V. Aksenov, Y. V. Nikitenko, K. Zhernenkov, B. Nagy, A. Teichert, R. Steitz, A. Rühm, and L. Bottyán, "Magnetic proximity effects in V/Fe superconductor/ferromagnet single bilayer revealed by waveguide-enhanced polarized neutron reflectometry," *J. Supercond. Nov. Magn* **24**, 961-968 (2011).<https://doi.org/10.1007/s10948-010-1041-0>
 18. Y. M. Shukrinov, I. Rahmonov, and K. Sengupta, "Ferromagnetic resonance and magnetic precessions in ϕ 0 junctions," *Phys. Rev. B* **99**, 224513 (2019).<https://doi.org/10.1103/PhysRevB.99.224513>
 19. I. Žutić, J. Fabian, and S. D. Sarma, "Spintronics: Fundamentals and applications," *Reviews of modern physics* **76**, 323 (2004).<https://doi.org/10.1103/RevModPhys.76.323>
 20. F. Konschelle and A. Buzdin, "Magnetic moment manipulation by a Josephson current," *Phys. Rev. Lett.* **102**, 017001 (2009).<https://doi.org/10.1103/PhysRevLett.102.017001>
 21. B. D. Josephson, "Possible new effects in superconductive tunnelling," *Physics letters* **1**, 251-253 (1962).[https://doi.org/10.1016/0031-9163\(62\)91369-0](https://doi.org/10.1016/0031-9163(62)91369-0)
 22. P. W. Anderson and J. M. Rowell, "Probable observation of the Josephson superconducting tunneling effect," *Phys. Rev. Lett.* **10**, 230 (1963).<https://doi.org/10.1103/PhysRevLett.10.230>
 23. A. A. Golubov, M. Y. Kupriyanov, and E. Il'ichev, "The current-phase relation in Josephson junctions," *Reviews of modern physics* **76**, 411 (2004).<https://doi.org/10.1103/RevModPhys.76.411>
 24. B. Li, R. V. Chopdekar, E. Arenholz, A. Mehta, and Y. Takamura, "Unconventional switching behavior in La_{0.7}Sr_{0.3}MnO₃/La_{0.7}Sr_{0.3}CoO₃ exchange-spring bilayers," *Appl. Phys. Lett.* **105**, 202401 (2014).<https://doi.org/10.1063/1.4902115>
 25. S. Koohfar, A. B. Georgescu, A. N. Penn, J. M. LeBeau, E. Arenholz, and D. P. Kumah, "Confinement of magnetism in atomically thin La_{0.7}Sr_{0.3}CrO₃/La_{0.7}Sr_{0.3}MnO₃ heterostructures," *npj Quantum Materials* **4**, 1-8 (2019).<https://doi.org/10.1038/s41535-019-0164-1>
 26. V. Lauter-Pasyuk, H. Lauter, B. Toperverg, L. Romashev, and V. Ustinov, "Transverse and Lateral Structure of the Spin-Flop Phase in F e/C r Antiferromagnetic Superlattices," *Phys. Rev. Lett.* **89**, 167203 (2002)
 27. C. G. Shull, W. Strauser, and E. Wollan, "Neutron diffraction by paramagnetic and antiferromagnetic substances," *Physical Review* **83**, 333 (1951).<https://doi.org/10.1103/PhysRev.83.333>

Dr. V. Zhaketov